Modelling ultraviolet exposures in a school environment

Nathan Downs,*[a] Alfio Parisi[a], Joanna Turner[a], David Turnbull[a]

[a] University of Southern Queensland, Darling Heights, Toowoomba, Australia. Fax: 61 7463 12721; Tel: 61 7463 12727; [*]E-mail: downsn@usq.edu.au

Abstract

A technique has been developed to represent erythemally effective ultraviolet radiation exposure within a school environment. The technique models the erythemally effective exposure onto a horizontal plane representation of a mapped school environment located in Hervey Bay (25^oS, 153^oE), Australia. The input parameters used to model the ultraviolet exposures received within the school playground included the measured sky view, ground albedo and standing surface albedo. Estimates of the erythemally effective ultraviolet exposure received within the school playground during morning tea and lunch time meal breaks during a winter and summer school day are presented. The influence of tree shade and building structure was found to vary significantly with solar zenith angle modelled over the winter and summer school meal break times with horizontal plane exposures predicted to vary from between 0 and 7 SED at different locations within the playground. The technique presented provides a method that can be followed to examine the effect of surrounding buildings and surface structures of real environments on the predicted horizontal plane ultraviolet exposure.

Introduction

The ultraviolet index, recently revised and adopted by joint recommendation of the World Health Organisation (WHO)[1], World Meterological Office (WMO), the United Nations Environment Programme (UNEP) and the International commission on Non-Ionizing Radiation Protection (ICNIRP), is perhaps the most well known representation of the predicted horizontal plane exposure relied upon by the public to assess exposure risk. The measured and modelled UV index, in addition to other methods used to represent UV exposure provides a reasonable first approximation of exposure likely to be received by subjects using outdoor environments. Often however, the influence of the surrounding environment is neglected, due to the time required, and difficulties in making accurate environmental measurements sufficient to detail all the factors that impact ambient UV. The influence of solar position and its effect on surface albedo[2,3], variation with sky view[4], and surface inclination[5,6] have each been investigated and modelled in past research, however no mechanism has yet been developed to take each of these factors into account to model horizontal plane damaging UV in a realistic environment. Additionally, horizontal plane damaging UV does not accurately represent exposure likely to be incident on exposed surfaces of the human body although many studies have been and continue to be conducted to investigate and model this effect.[7,8,9,10,11,12]

In Australia, more effective population measures of sun exposure were called for by the National Health and Medical Research Council's (NHMRC) Sun Protection Programs Working party.[13] Recently, the various state cancer councils have recommended the adoption of guidelines outlining better policies in regards to the formal provision of shade, use of hats, protective clothing, sunscreens and limiting of personal exposures during periods of peak solar UV irradiance. These recommendations promoted through various campaigns, have led to an increasing awareness of sun safe practices among the general public[14] and standards required for the provision of safe working and recreational environments that cover sunscreen use, clothing and eyewear protection and shade provision have been published in Australia.[15,16,17,18] However, attitudes and behaviours by many members of the general public have often been slow to take up the sun safe message. Previous studies involving school children have shown that less than one third practice effective sun protection in the United States[19] with similarly low sun safe attitudes and behaviours being observed by adolescents in Australia.[20] For school aged children, being a significant risk group for the development of solar induced disease[21,22,23] and being placed in school environments during periods of peak solar UV irradiance, the need to understand the local school environment and the UV interactions within that environment is an important step in reducing the risks associated with exposure to UV. This research addresses the need to develop a method that can be used to assess UV exposure risk to students in school playgrounds by using a photographic technique to survey individual environments.

Materials and methods

The erythemally effective ultraviolet (UV$_{ery}$) in a school playground has been estimated from measurements of sky view and modelled predictions of the UV$_{ery}$ due to the measured local surface albedo and estimated solar position. A single

school playground was studied in sub tropical Queensland, located in Hervey Bay (25°S,153°E). Variation in modelled predictions of the horizontal plane playground UV_{ery} with changing Solar Zenith Angle (SZA) has been estimated for the morning tea and lunch time meal breaks of 21 June and 13 December 2008. These dates were chosen to represent the winter solstice (21 June 2008) and last day of the school year observed in Queensland (closest day to the summer solstice, 13 December 2008) and taken to be the break periods of the school year during which students would experience minimum and maximum exposure to UV_{ery}. The dates are hereafter referred to as WS (winter solstice for the year 2008) and SS (sumer solstice for the year 2008). Measurements of the sky view at the studied location were used to determine the diffuse and direct UV_{ery} components incident on a horizontal plane. The technique presented could similarly be applied to any real environment for which estimates of the UV_{ery} are required. Modelled estimates of the horizontal plane UV_{ery} were calculated using a hybrid model developed previously.[24] The horizontal plane UV model utilises input parameters that include SZA, for the specific latitude, longitude and time of year, altitude, ozone concentration, aerosol optical depth, and cloud cover. For the research presented here, variation with cloud cover, altitude, and various atmospheric parameters including variation in ozone were not considered.

Study location

A total of 57 sites located at Hervey Bay State High School were photographed in a series of two straight survey lines taken parallel to the school's western facing fence. The region studied covered an area approximately 170 m long and 15 m wide. A diagrammatic representation of each of the 57 photographed sites within the study region is shown in Figure 1. Sites were separated by approximately 5 m and photographs were taken where practically possible at this incremental level. Where photographs could not be taken, due to obstructions, sites were selected to be as close as possible to the intended location to maintain a 5 m separation. The choice of 5 m was taken to provide approximately 31 measurement sites along both site survey lines measured with respect to the school's western fence line and was found to be of small enough separation to detail significant variation in the sky view as observed from the ground.
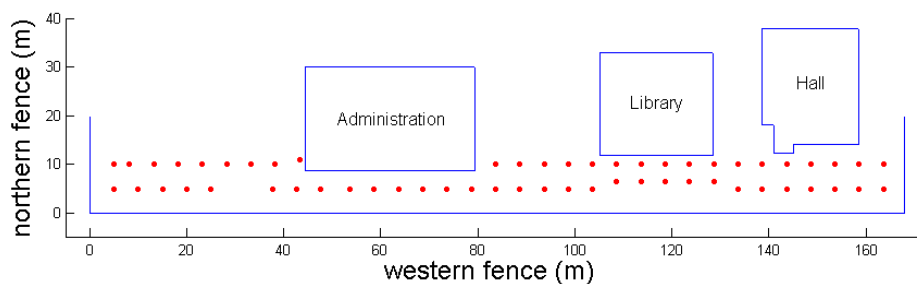
Fig. 1 Survey site locations for the sky view and estimated UV_{ery} environmental exposure measured inside part of the playground of Hervey Bay State High School.

Sky view

Image field and classification.

Measurements of the sky view were taken by application of an image processing algorithm to classify sky regions from the local surface environment for a ground observer. A series of 16 images were taken at each of 57 sites in the school playground to form single composite site images using a Digital SLR camera (50 mm lens) at f11 (Canon EOS 350D). The camera was orientated at 0° and 30° to the horizon with the respective composite image covering a SZA range of 32° to 90° and 0° to 360° in azimuth. The camera was fitted to a tripod, and positioned with respect to North at a height of 1 m.

A composite image measurement of the sky view at each playground site was used as the preferred method over an upward facing fish eye lens in order to minimise distortion of surface objects which required later image classification. The sky view less than 32° in SZA was predominately clear of surface obstructions in the playground. Sites that were covered by surface objects above this range were noted upon survey of the study site and estimates of sky view above this range were included in total sky view measurements. For measurements of the sky view presented here, two shade structures were found to cover the sky above 32° in SZA and for these cases the percentage of cover above 32° was estimated.

The image processed sky view was determined as the percentage of pixels classified as "sky" in each site composite image and included the sky view estimate for a SZA less than 32°. For the image processing algorithm, the difference between the blue and red (B-R) RGB colour level of each pixel in the unprocessed photograph of each composite playground site was used to determine if an image pixel would be classified as "sky" or surface obstruction. Pixels having a higher blue RGB level in unprocessed photographs produce a positive B-R difference. For an unprocessed image pixel to be classified as a "sky" pixel by the image processing algorithm used here, the RGB blue level needed to be significantly higher than the respective RGB red pixel level. For this research, the threshold B-R value was set at 0.85, which classified the majority of sky pixels seen in the unprocessed photograph as can be observed by comparing the processed site composite image to the original photograph (Figure 2). In the figure, pixels classified as "sky" were given the false colour blue, remaining pixels were classified as surface obstructions and coloured white. Due to atmospheric scattering, particularly at low solar elevations, the red component of unprocessed RGB pixel levels made the classification of "sky" pixels difficult if a B-R threshold of 1 was used (pixels containing no RGB red colour level). For different locations and other research applications the B-R threshold should be changed to suit the sky light conditions of the location. Furthermore, such a technique used to classify sky view does not distinguish between white cloud and surface objects in the unprocessed photograph and is similarly limited if blue surface objects are photographed in which case these may need to be manually edited from the image before processing. Images used for this study were taken on days with no cloud cover. Figure 2 shows a single image before (bottom) and after (top) image processing taken in the north western corner of the playground. The sky view in the processed figure, determined as the percentage of pixels classified as "sky" relative to the unobstructed sky view was calculated in this case to be 77%. The complete processed sky view determined from photographs taken at each of the 57 playground study sites and expressed as a percentage of an unobstructed sky view is given in Figure 3. Note in Figure 3 that at 10 m from the western fence line, the

survey is obstructed by the school administration building resulting in 0% sky view between approximately 50 m and 80 m.
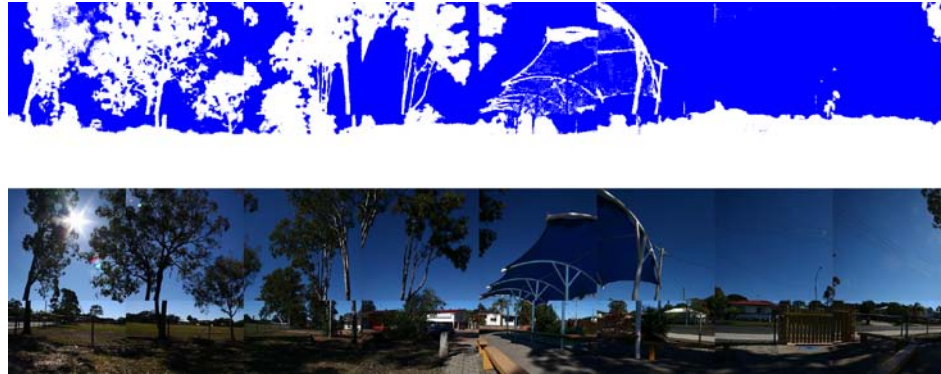
Fig. 2 Composite site image and processed sky view image photographed in the north western corner of the playground study site. In the top false colour image, the sky is coloured blue while surface obstructions are coloured white. An image mask was used to separate the unobstructed horizon from the ground for calculation of the sky view percentage.
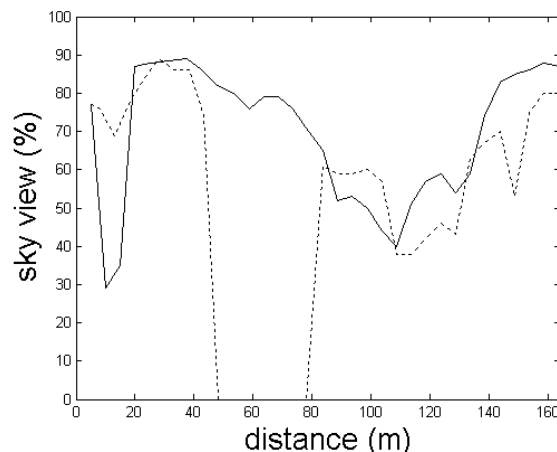
Fig. 3 Variation in sky view along each survey line measured at Hervey Bay State High School at 5 m from the western fence (solid line) and 10 m from the western fence line (dashed line).

Solar position and calculating erythemally effective site UV.

The position of the sun in altitude and azimuth was calculated[25] and superimposed onto each of the 57 processed site composite images for the morning tea (11.25 to 12.05) and lunch (13.15 to 13.55) meal break times observed at the school for WS and SS. Figure 4 shows the superimposed position of the sun for each of these times for one site imaged within the playground. Positioning of the solar disk within the composite image was calculated by determining the number of image pixels each degree represents in both SZA and azimuth. In azimuth, 5.4 pixels per degree (image width 1994 pixels) were used to represent positions ranging from the photographed true north position of 0° (image left) to 360° (image right). The

number of pixels per degree varied with SZA. For the SZA image positions used in this research, 4.1 pixels per degree were used for the top 118 image pixels. This covered the SZA range less than 58.5$^\mathrm{o}$ and was the range used to plot the winter SZA position experienced during both the WS morning tea and lunch break times. In the summer SZA range however, the solar position is placed beyond the composite image field of view. The degree of cover in these cases was estimated at each position based on the information that could be obtained from the plotted azimuth solar position and observer notes of cover for a SZA less than 32$^\mathrm{o}$ (the photographed image limit) made during the sky view survey.

The direct and diffuse UV$_{\mathrm{ery}}$ was calculated for each of the 57 composite site images taken over the playground study site. Table 1 provides the erythemally effective direct and diffuse UV$_{\mathrm{ery}}$ irradiance estimated for the site pictured in Figure 2. Estimates of the UV$_{\mathrm{ery}}$, integrated over intervals of 5 minutes were modelled by weighting the global spectral ultraviolet, S over the 280 nm to 400 nm range to the human erythemal action spectrum, A[26]:

$$\mathrm{UV}_{\mathrm{ery}} = \int_0^T \int_{UV} \mathrm{S}(\lambda,\mathrm{t})\mathrm{A}(\lambda)\mathrm{dtd}\lambda \qquad (1)$$

Modelled UV$_{\mathrm{ery}}$ contributions provided in Table 1 are given for the end of each 5 minute interval, therefore null estimates of exposure are provided at break start times in the Table. Where the solar disk was obscured by a surface object, the direct UV$_{\mathrm{ery}}$ contribution was given as 0 Jm^{-2} as can be noted from the Table for the winter morning tea exposure interval between 11.55 and 12.05. Here, surface obstruction of the solar disk at any particular playground site was determined by comparison of each of the 57 processed site images with the superimposed position of the sun plotted for each of the meal break times as per Figure 4. Diffuse UV$_{\mathrm{ery}}$ irradiance was further weighted to the percentage estimate of sky view at each playground site. Diffuse UV$_{\mathrm{ery}}$ provided in Table 1 was weighted to an estimated 77% sky view.

Negating the effect of site obstruction to the direct and diffuse UV$_{\mathrm{ery}}$, morning break exposures were predicted to be higher than lunch break exposures due to the decreasing altitude of the sun with respect to the observed school break times. Subsequently the relative proportion of direct UV$_{\mathrm{ery}}$ is lower than diffuse UV$_{\mathrm{ery}}$ at lunch break times observed at this school than during morning tea break times. Furthermore, the direct proportion of UV$_{\mathrm{ery}}$ is lower during WS than SS break periods due to the lower altitude of the sun and the subsequent increased absorption of direct UV$_{\mathrm{ery}}$. For the two seasonal periods modelled here, the unobstructed ratio for direct to diffuse UV$_{\mathrm{ery}}$ varied from 0.60 to 0.53 between the respective WS morning tea and lunch break times and from 0.92 to 0.82 between the respective SS morning tea and lunch break times. The influence of site structure affecting the relative proportion of direct and diffuse UV$_{\mathrm{ery}}$ is cleary evident in Table 1 particularly during SS break times when unobstructed direct UV$_{\mathrm{ery}}$ exceeds the sky view weighted diffuse UV$_{\mathrm{ery}}$. The erythemal weighting of the modelled UV significantly influences the direct UV$_{\mathrm{ery}}$ in high afternoon SZA ranges as is evident in the above unobstructed direct to diffuse ratios. Increases in afternoon UVA are negated by weighting with the erythemal action spectrum, consequently the decreases in the afternoon UV$_{\mathrm{ery}}$ modelled here are due in part to the increased erythemal dependence on shorter UVB wavelengths.

Fig. 4 Solar position during morning and lunch meal break times for a single site photographed in the north western corner of the playground. (Green downward arrow – WS morning tea solar position; Yellow downward arrow - WS lunch time solar position; Green upward arrow – SS morning tea azimuth solar position, Yellow upward arrow – SS lunch time azimuth solar position).

Table 1 Five minute horizontal plane direct and diffuse UV_{ery} exposure modelled for each of the morning and lunch meal break times calculated for WS and SS for the playground site shown in Figure 4.

Time	Winter (morning tea)		Summer (morning tea)		Time	Winter (lunch break)		Summer (lunch break)	
	Direct (Jm^{-2})	Diff. (Jm^{-2})	Direct (Jm^{-2})	Diff. (Jm^{-2})		Direct (Jm^{-2})	Diff. (Jm^{-2})	Direct (Jm^{-2})	Diff. (Jm^{-2})
11.25					13.15				
11.30	10.3	13.4	45.7	38.2	13.20	7.5	10.6	36.3	33.0
11.35	10.4	13.5	45.9	38.3	13.25	7.2	10.3	35.3	32.4
11.40	10.5	13.5	46.0	38.4	13.30	6.9	9.9	34.3	31.8
11.45	10.5	13.6	46.0	38.4	13.35	6.6	9.6	33.3	31.2
11.50	10.6	13.6	46.0	38.4	13.40	6.3	9.2	32.3	30.5
11.55	0	13.6	45.9	38.3	13.45	5.9	8.9	31.3	29.9
12.00	0	13.6	45.7	38.2	13.50	5.6	8.5	30.2	29.2
12.05	0	13.5	45.5	38.1	13.55	5.3	8.1	29.1	28.5
Total	**52.3**	**108.3**	**366.7**	**306.3**	Total	**51.3**	**75.1**	**262.1**	**246.5**

Notes on modelled horizontal plane playground exposures

The global horizontal plane UV_{ery} exposure was modelled at each of the 57 playground sites. Global UV_{ery} included a direct and diffuse component as modelled in previous research[24] with the exception of weighting to site sky views. For this research, the modelled diffuse UV_{ery} was weighted to each of the respective 57 site sky views. Direct UV_{ery} was included in global exposure estimates at each site only if the solar disk was not obstructed by surface objects. Exposures were modelled as those contributions that are normally incident to a horizontal plane (*i.e.* vertically incident radiation). Contributions to site global UV_{ery} irradiance, due to standing and ground surface albedo discussed in the following sections are likewise those contributions that influence the vertically incident radiation only. In the determination of diffuse albedo contribution, vertically incident atmospheric backscatter due to ground surfaces was calculated. Direct UV_{ery} albedo contribution was calculated as the component that is vertically incident to a horizontal plane caused by standing surface objects. Therefore, albedo contributions to the global UV_{ery} were determined at each of the 57 playground sites depending on the predominant ground surface for diffuse contributions, and the average albedo of surrounding standing surfaces for the direct contribution.

Calculations of the UV_{ery} irradiance were performed for clear skies only and

contributions to the diffuse UV_{ery} due to vertical surface reflections were not calculated. Ozone was assumed to be consistent at 320 Dobson units (DU) and aerosol and extinction amounts were implemented with parameters specified as discussed in the sections that follow. It is assumed that the measured standing surface albedo will be the same with variation in SZA. The direct standing surface albedo contribution (A_{dir}) was not calculated for shaded playground sites, where shading was determined by the modelled position of the sun with respect to surface obstructions indicated within processed site images.

The choice of 320 DU used in this model was taken to represent the maximum likely ozone concentration observed over the study site. Maximum ozone concentrations in June and December 2007 varied from between 303 DU to 297 DU respectively.[27] The modelled exposures provided for this research therefore represent the minimum likely environmental UV_{ery} under clear sky conditions.

Comparison between 107 spectral irradiance measurements recorded in 5 minute intervals on a single clear day at the University of Southern Queensland (model DTM300, Bentham Instruments, Reading, UK) to the modelled horizontal plane clear sky UV_{ery} irradiance using the hybrid model presented here for a SZA range less than 60° indicated that the modelled irradiance was lower than the measured irradiance by 7%±6% (1σ) for an equivalent ozone concentration of 251 DU measured over the comparison day[27]. The overall uncertainty of the measured spectroradiometer irradiance employed in this comparison, traceable to the UK National Physical Laboratory standard, is estimated at ±9%[28] giving the total uncertainty in the modelled horizontal plane irradiance at 16% negating variation in ozone concentration. The composite site image limit of 32° in SZA increases the uncertainty in modelled horizontal plane exposure when coupled with the model uncertainty of 16% for the SS morning tea and lunch break times. Here, 38 of the 57 playground sites were noted to be obstructed above the image limit of 32° in SZA predominately by tree cover. The region of sky not able to be photographed makes up 36% of the total sky view. The additional uncertainty caused by this estimate of cover in this range and its effect on the modelled direct and diffuse UV_{ery} is therefore likely to be significantly less than 36% and is dependent on the accuracy of the observer.

Surface albedo contribution to the modelled UV_{ery}

Ground and standing surface albedo measurement.

The surface albedo contribution at each playground site was measured and used to model the downward horizontal plane UV_{ery} exposure. Contributions to the direct and diffuse UV_{ery} exposure were modelled for both ground and standing surfaces at each of the 57 playground sites. Surface albedo contributions were modelled for bitumen, concrete, paving, grass, brickwork, painted brickwork, and standing vegetation. The albedo of each of these surfaces was determined as the ratio of global UV_{ery} to reflected UV_{ery} measured at a distance of 0.5 m from ground and vertical standing surfaces. Reflected albedo measurements of UV_{ery} were taken orientated along the surface normal for both ground and standing vertical surfaces. Standing surface albedo was further measured with respect to azimuth orientation. Measurements of ground surface albedo were performed in the playground using a handheld Robertson-Berger meter (Solar Light Co., Philadelphia, PA 19126).

Vertical standing surfaces were measured with a spectrometer (EPP2000, Stellarnet, Florida, USA). The albedo of ground and standing vertical surfaces found over the playground study site are listed in Table 2. Where data is not included in the table, such facings were not present in the playground study area.

Table 2 Albedo of ground and standing surfaces found in the playground.

Ground Surfaces	Albedo (%) at 0.5 m			
Bitumen	6			
Concrete	6			
Pavers	5			
Grass	2			
	Albedo (%) at 0.5 m			
Standing Surfaces	North Facing	East Facing	South Facing	West Facing
Painted brickwork	7	7	3	1
Brickwork	2	4	-	1
Standing vegetation	4	2	-	-

Modelling site albedo contributions.

Ground surfaces and modelling diffuse UV_{ery} contribution.

Contributions to the diffuse UV_{ery} due to site ground surfaces were modelled according to the surface albedo downward diffuse UV atmospheric backscatter[29,30,31]:

$$U_{diff} = V(H(\lambda)e^{-D_t(\theta,\lambda)} + A_{diff}) \qquad (2)$$

$$A_{diff} = r(\lambda)S \qquad (3)$$

$$S = \frac{A_s G E}{1 - r(\lambda)A_s} \qquad (4)$$

Where U_{diff} is the modelled horizontal plane diffuse UV, A_{diff} is the modelled albedo contribution to the downward diffuse UV irradiance, and V is the site sky view. S is the surface albedo UV irradiance, G, is the global UV irradiance, E is an altitude dependent parameter, and A_s is the site ground surface albedo measured at 0.5 m. The terms $H(\lambda)$, $r(\lambda)$ and $D_t(\theta,\lambda)$ represent the extra terrestrial irradiance, atmospheric air reflectivity and altitude dependent variation in aerosol optical depth and concentration respectively. These terms are dependent on wavelength, λ across the 280 nm to 400 nm UV waveband and SZA, θ. The detail of equation (2), particularly the term $D_t(\theta,\lambda)$ is adequately described[31] and has been discussed previously.[32]

Standing surfaces and modelling the direct UV_{ery} contribution.

Contributions to the direct UV_{ery} due to standing surfaces were modelled according to the equations:

$$U_{dir} = \mu H(\lambda)e^{-A_t} \qquad (5)$$

$$U_{dirA} = U_{dir} + A_{dir} \qquad (6)$$

Here, μ is the cosine response, and A_t the attenuating atmospheric thickness of air, aerosol and ozone species elsewhere described in detail.[33,32] U_{dirA} is the modelled direct UV component of the global UV irradiance (direct vertical component), and A_{dir} is the vertical cosine component of direct UV due to the standing surface albedo which is dependent on A_s, the measured standing surface albedo (eqn 7). The global direct component of the UV irradiance (U_{dir}) was formulated in this instance as the cosine of the sun normal direct UV (Figure 5). The direct component of standing surface albedo, A_{dir}, takes the same value as the product of the standing surface albedo (A_s) and the cosine of the sun normal UV, U_{sn}, giving an equation dependent on U_{dir}, the direct UV irradiance and the standing surface albedo:

$$A_{dir} = A_s U_{sn} \cos(SZA)$$
$$A_{dir} = A_s \frac{U_{dir}}{\cos(SZA)} \cos(SZA) \qquad (7)$$
$$A_{dir} = A_s U_{dir}$$

Note as previously mentioned, that for this study, only the downward vertical contributions of the direct (A_{dir}) and diffuse (A_{diff}) albedo were applied to a modelled horizontal plane surface in the playground area.
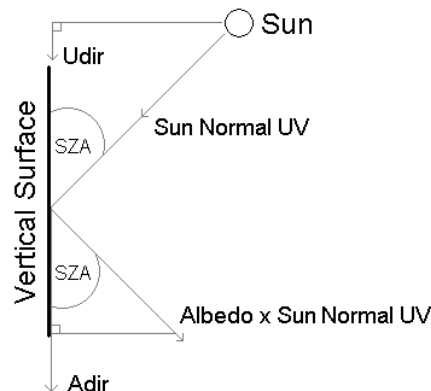
Fig. 5 Schematic representation of the direct albedo UV contribution, A_{dir}, modelled for vertical standing surfaces.

Determination of site standing surface albedo contribution.

Composite site images were examined to determine the relative area of vertical standing surfaces orientated with respect to North, East, South and West. Composite images were divided into four segments to approximate regions of surface orientation. Each region was classified as either clear (no albedo contribution), painted brickwork, brickwork or standing vegetation and an average standing surface albedo value was calculated for each playground site. Figure 6 above shows how site standing albedo contributions were calculated for a site located near the school library. Vertical standing structures, including both vegetation and buildings that were further than 5 m from the playground image location were classified as "clear" for the calculation of standing site albedo.

Fig. 6 Standing surface albedo contribution estimate for a site located near the school library. The total site contribution of A_{dir} (0.0075) was estimated from the average of 0 for a clear south facing region (image left), 0.01 for painted brickwork west facing (mid left image), 0 for the predominately clear north facing region (mid right) and 0.02 for east facing standing vegetation (image right).

Results

Contour variations in the UV_{ery}

Variation in the modelled surface UV_{ery} was determined along both survey contour lines in the playground study area. The modelled horizontal plane UV_{ery} exposure varied according to site sky view, SZA and site albedo contribution. Site sky view and SZA were the most significant factors influencing the predicted horizontal plane playground UV_{ery} exposure. Figure 7 shows the predicted playground UV_{ery} exposure predicted along the 5 m and 10 m survey lines parallel to the school's western fence estimated over the morning and lunch meal break times for WS and SS before the addition of the surface albedo contribution. Exposures are provided in units of Standard Erythemal Dose (SED) where an SED is defined as 100 Jm^{-2} of erythemally effective UV.[34] The most significant features evident in Figure 7a are the curve dips located at approximately 10 m and 110 m, these were due to reductions in sky view caused by a bus shelter and overhead tree shade respectively. The influence of the bus shelter and tree shade on UV_{ery} were reduced along the 10 m survey line as is evident in modelled UV_{ery} exposures at 10 m and 110 m in Figure 7b . The general shape of each of these curves closely resemble measured site sky view given in Figure 3, however the influence of surface structures with changing solar position modifies the curves during different meal break times. The effect of surface structure in the playground significantly varies the shape of the curves from the sky view curve observed in Figure 3 during the studied winter meal break times. Variation in the winter meal break time curves from the sky view contour curves of Figure 3 indicate that winter time exposures are less dependent on sky view. This is because the direct UV incident from a lower elevation blocked by surface structures has more influence on the total modelled global UV_{ery} plotted in the figure, altering the shape of the exposure curve from the sky view curve more than is observed in summer due to high solar elevation removing the influence of surface structure. Significantly, Figure 7 clearly identifies that the intensity in playground exposure is also less variable during winter meal break times and significantly lower than respective summer meal break times with the average combined morning tea and lunch exposures measured over each of the 57 playground sites varying from between 1.2±0.5 SED (1σ) to 4.8±1.8 SED (1σ) between winter and summer breaks respectively.
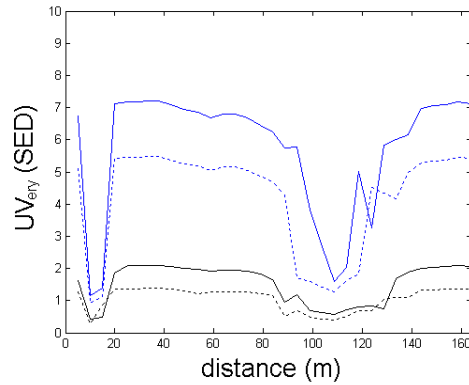
Fig. 7a 5 m contour line showing variation in the global UV_{ery} plotted for morning tea (solid) and lunch time (dashed line). Exposures are modelled for WS (black) and SS (blue).
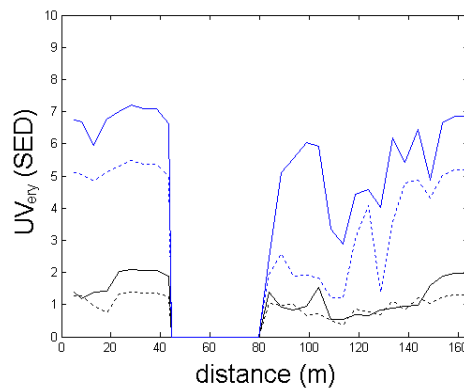

Fig. 7b 10 m contour line showing variation in the global UV_{ery} plotted for morning tea (solid) and lunch time (dashed line). Exposures are modelled for WS (black) and SS (blue)

The influence of site albedo

The direct and diffuse albedo weighted contributions to the horizontal plane UV_{ery} are included for comparison with the unweighted UV_{ery} exposure provided in Figure 7. Figure 8 clearly identifies locations in the school playground where the UV_{ery} is increased due to the influence of the local environment surface albedo. The albedo contributions to the modelled direct and diffuse UV_{ery} given in Figure 8 were modelled for each of the 57 sites in the playground during both summer and winter meal break times. Peak variations evident in the Figure are due to high surface albedo and significant contributions due to north facing standing vegetation and north facing painted brickwork. UV_{ery} exposures to children at these locations within the playground are likely to be higher than the model predictions provided here, given surface reflections have been modelled for a horizontal plane only. The use of comparative modelling between the albedo and unweighted albedo contribution to the UV_{ery} identifies regions in the playground that enhance exposure risks to students due to the surrounding environment.
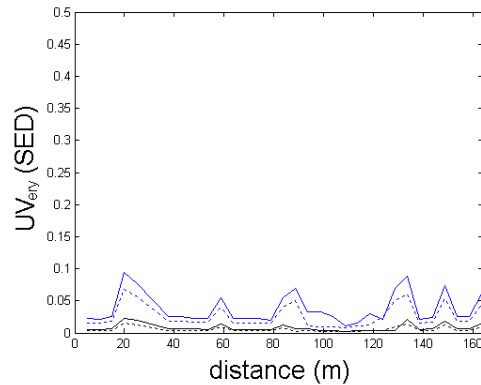
Fig. 8a Increase in modelled UV_{ery} due to ground and standing surface albedo contribution expected along the 5 m survey line plotted for morning tea (solid) and lunch break times (dashed). Exposure contributions are modelled for WS (black) and SS (blue).
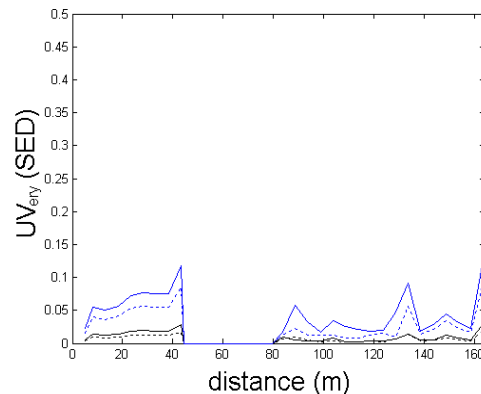

Fig. 8b Increase in modelled UV_{ery} due to ground and standing surface albedo contribution expected along the 10 m survey line plotted for morning tea (solid) and lunch break times (dashed). Exposure contributions are modelled for WS (black) and SS (blue).

Modelling surface area UV_{ery} from site data

The global UV_{ery} exposure modelled at each playground site and given in Figure 7 has also been presented with respect to the surface area covered in the survey for each of the morning tea and lunch break times for WS (Figure 9) and SS (Figure 10). Surface area exposures were represented as contour maps generated using MATLAB (The MathWorks, version 7). Linear interpolation was used to generate the surface map contours illustrated in the Figures. The resulting contour plots highlight regions of peak UV intensity on a scaled map of the studied playground for each of the morning and lunch meal break times.

Modelled horizontal plane exposures in Figures 9 and 10 varied from between 0.3 SED to 7.2 SED. These results are in good agreement with mean vertex measurements previously recorded over hourly periods at the same school in an open environment. During a 12 month study run between 2006 and 2007, the calibrated mean vertex UV_{ery} varied from between 0.9 SED to 7.8 SED.[35]
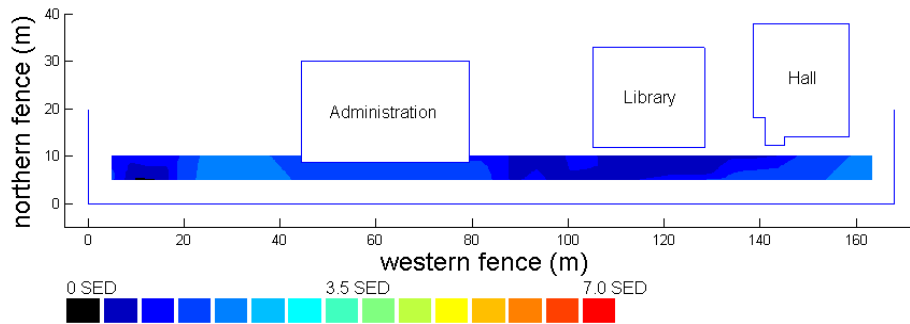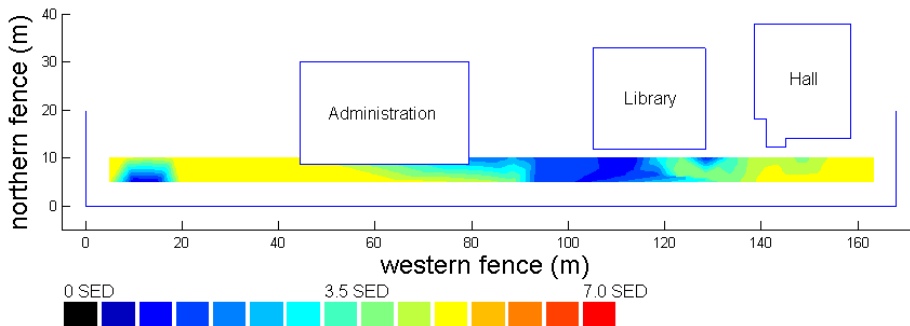
Fig. 9a Contour plot of the horizontal plane UV$_{ery}$ exposure for the school morning tea break time (11.25-12.05) occurring at WS.
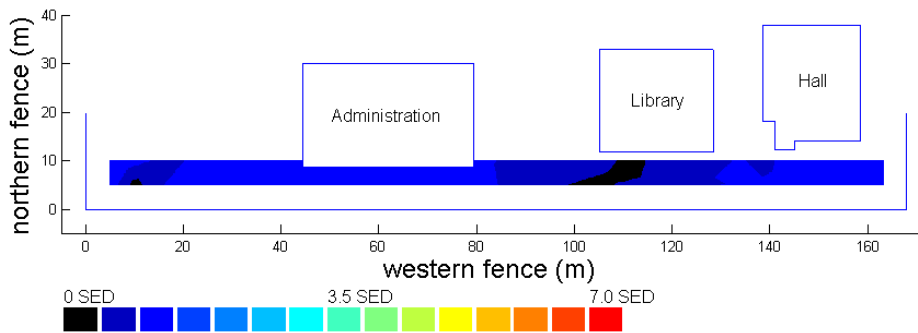
Fig. 9b Contour plot of the horizontal plane UV$_{ery}$ exposure for the school lunch break time (13.15-13.55) occurring at WS.
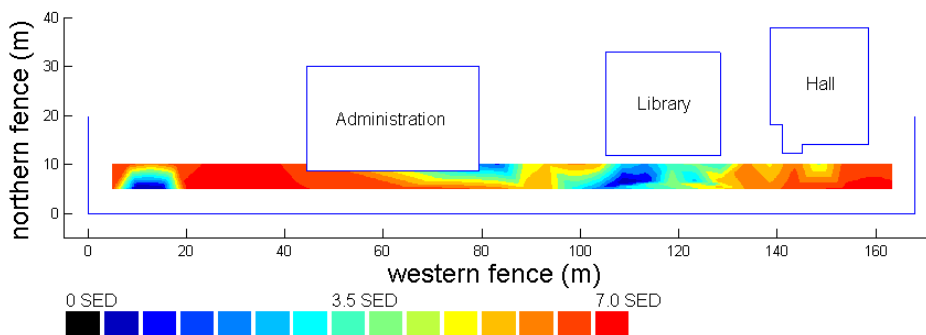
Fig. 10a Contour plot of the horizontal plane UV$_{ery}$ exposure for the school morning tea break time (11.25-12.05) occurring at SS.

Fig. 10b Contour plot of the horizontal plane UV$_{ery}$ exposure for the school lunch break time (13.15-13.55) occurring at SS.

Shade structures in the modelled environment

In each of the playground exposures illustrated in Figures 9 and 10, the influence of a small bus shelter (Figure 11) can be seen at approximately 10 m. UV_{ery} exposures modelled using the technique developed for the school bus shade structure presented in this research are comparable with subsequent protection factors (PF) measured for similarly built shade structures placed in a open environment.[36] Here, sky view images were taken underneath the bus shade structure along the first survey line at 10 m and 15 m from the school's northern fence. The sky view at these locations was determined to be 30% and 36% respectively which included an estimated 14% transmittance factor for UV penetration through the bus shelter's blue PVC shade cloth cover.[37] Both covered survey sites were approximately centered underneath the bus shade structure shown in Figure 11. The reduction in modelled UV_{ery} exposure along the survey line passing through the bus shelter structure is listed in Table 3. The estimated PF for the shelter was determined as the ratio of modelled unprotected UV_{ery} to the protected UV_{ery} values listed in the table. The estimated PF for the structure in this school playground although varying with the different school meal break times is similar to measured PFs of 1.8-16.1 determined for shade cloth,[38] PFs of 4-8[39] determined for shade structures located in New Zealand primary schools and PFs found for small sized shade structures determined at < 3 in winter and < 8 in summer.[36]

Fig. 11 The playground bus shelter significantly reduced modelled UV_{ery}.

Table 3 Survey line variation in UV_{ery} exposure modelled about the bus shelter for morning and lunch meal break times. Estimated PF was calculated using the ratio of average unprotected modelled UV_{ery} to average protected modelled UV_{ery}

Distance from northern fence (m)	Morning tea (WS)	Lunch (WS)	Morning tea (SS)	Lunch (SS)
5	1.6 SED	1.3 SED	6.7 SED	5.1 SED
10*	0.4 SED	0.3 SED	1.2 SED	0.9 SED
15*	0.5 SED	0.9 SED	1.4 SED	1.1 SED
20	1.9 SED	1.4 SED	7.1 SED	5.4 SED
Estimated PF	4	2	5	5

[a] Survey sites marked with an (*) were located underneath the bus shelter.

Tree shade in the modelled environment

The image processing technique applied throughout this research adequately assesses the quality of tree shade, providing estimates of the degree of cover

provided by different trees found in the playground. As expected, thicker trees were found to more likely block the direct UV irradiance and subsequently influence the modelled UV_{ery} exposure than trees that provided less cover. Comparison of solar position with image processed tree structure provided a simple and useful method of assessing tree shade quality allowing its influence to be plotted over a horizontal plane. The influence of thick tree cover, prominent along the school's western fence between 90 m and 130 m and sparse tree cover provided in the north-western corner of the school playground is clearly evident in each of Figures 9 and 10.

Fig. 12a North facing view of sparse cover located in the north western corner of the surveyed school playground.

Fig. 12b North facing view of thick tree shade located between 90 m and 130 m.

Measurements of the horizontal plane UVB (320 nm to 280 nm) made underneath a tree grove in previous research[40] over the SZA range of 20°-50° indicates that irradiance relative to an open sky environment varies between 0.4 and 0.6 for sky views between 40% and 60%. Here, for tree cover between 90 m and 130 m the measured sky views taken along both survey contours ranged between 38% and 63% resulting in a UV_{ery} irradiance relative to an open environment of 0.42 and 0.45 (the equivalent of an approximate PF of 2) for SZA ranges of 21°-30° and 48° estimated for the summer lunch and winter morning tea breaks respectively. Measurements by other researchers[41] however, indicate that tree shade protection is more effective in the UVA wavelengths (320 nm to 400 nm) and direct comparisons between UVB estimates[40] may better be represented if they are reduced slightly to account for the increased UVA wavelength dependence of the erythemally effective UV modelled here. Modelled predictions of the playground horizontal plane UV_{ery} exposure in the school's shaded regions however compare well with measurement studies[42] for which the relative UV irradiance was determined at 0.42 in the SZA range 30°-54° under dense tree shade. Comparison

with measured results indicates that the technique presented here can be used to assess the quality of tree shade in realistic environments.

Conclusions

This paper has presented a technique to derive playground UV_{ery} exposures based on image processed measurements of sky view and albedo contribution in a real school environment. Such a technique provides a valuable contribution in determining areas of risk in real environments and can be used to asses both the long and short term effects of solar ultraviolet exposure on a horizontal plane or weighted to human body surfaces. Continuing research being conducted at Hervey Bay State High School involving the dosimetric measurement of erythema exposure is currently being collected and the technique presented here will be used to predict the weighted three dimensional exposure to the face, neck, arm, hand and leg of school children within the entire school playground environment. In the context of this research, lunchtime exposures were predicted for periods of minimum and maximum solar ultraviolet irradiance for the 2008 school year. Estimates of the morning tea and lunch time UV_{ery} exposure determined for this school were made for clear sky conditions assuming a consistent ozone concentration of 320 DU and minimal aerosol concentrations. Modelled exposures for this school are therefore likely to be modest underestimates of the actual exposure received by school children in southern Queensland. Nevertheless, summer time morning tea and lunch break exposures predicted here exceed the adopted National Heath and Medical Research Council's safe daily limit[15] of 30 Jm^{-2} across all regions of the studied playground. During winter, the safe daily exposure limit was exceeded for each of the morning tea and lunch breaks for most playground regions with the limit being exceeded across all playground regions provided children are likely to be spending both winter morning tea and lunch breaks in the playground as would seem reasonable on cool days when spending more time in the sun is likely to be desirable. These findings highlight that no outdoor regions of the school playground could be considered safe environments. Sun protective strategies, including the active use of hats, sunscreens and outdoor exposure limits should be implemented to reduce overexposure to the environmental $UV_{ery.}$

Recently, the risks of underexposure to ambient solar UV has been linked to the development of diseases including rickets,[43] type I diabetes,[44] multiple sclerosis[45] and the possible development of some cancers.[46,47,48] These risks are related to vitamin D deficiencies caused by limitations in diet, and the sunlight induced epidermal reaction of 7-dehydrocholesterol into pre-vitamin D_3.[49] At the latitude examined here, the biological response of vitamin D_3 production in human skin exceeds the predicted erythemally effective UV. This is due to the vitamin D_3 response having a greater weighting at shorter UV wavelengths than the erythemal response. Higher solar elevations observed at sub tropical latitudes result in less atmospheric scattering of the direct UV irradiance inducing a greater vitamin D_3 response than the observed erythema or sunburn reaction. The research presented here, although not specifically weighted to the vitamin D_3 response, suggests outdoor playground exposures received by Queensland school children present a much more significant risk for the development of skin cancers caused by overexposure than diseases linked with underexposure to UV. However, a useful

technique applied using a similar method as described for this research could be used to examine the regions of low vitamin D_3 effective UV in outdoor environments when weighted to the vitamin D_3 response of human skin, rather than the erythemal reaction.

UV_{ery} exposures modelled in the playground for this paper included examination of the effectiveness of an open bus shelter and tree shade. These two regions combined with sky view measurements taken at each of the 57 playground sites showed some variation in the degree of protection provided both in the modelled UV_{ery} intensity and the variation in protected ground surface pattern. These variations were linked strongly to site sky view and direct UV irradiance influenced by local site structures. In order to make accurate assessments of the UV_{ery} in a realistic environment such as the school playground modelled here, variation in surface UV irradiance with solar position relative to the environment should be considered. Predictions of the open environment surface UV intensity such as the widely available UV index reported frequently by local forecasting agencies do not take such considerations in account, showing typically variation in UV irradiance due only to seasonal effects. While such predictions are a valuable guide to assessing the general UV risk, more detailed assessments taking the local environment into account, such as that applied here, can provide better information to the public, education and health authorities to better plan and assess for risks likely to be incurred by those using outdoor environments. This may include better planning of schedules for outdoor activity, the organisation of activity positions within a playground environment such as seating, or the assessment of regions of risk for determining positions of playground equipment, shade and other structures.

It was found here, that the largest variations in playground exposure occurred during the summer break times with the local environment playing a more significant role in the distribution of playground UV_{ery} than in winter due to more consistent variation in solar position. Planning of meal break times around periods of the day that show more consistent trends in playground UV_{ery} exposure would reduce exposures likely to be received by children while at school. It may be observed here for instance that lunch break exposures were lower than respective morning tea break exposures. Planning for an earlier morning tea break or substituting the morning break for a later afternoon tea break could have a significant impact on reducing the likely received UV_{ery} exposure.

Acknowledgements

Notes and references

1. WHO (World Health Organization), Global solar UV index: a practical guide, WHO, Geneva, Switzerland, 2002.
2. P. Weihs, Influence of ground reflectivity and topography on erythemal UV radiation on inclined planes, *Int. J. Biometeorol.*, 2002, **46**, 95-104.
3. G. Schauberger, Model for the global irradiance of the solar biologically-effective ultraviolet-radiation on inclined surfaces, *Photochem. Photobiol.*, 1990, **52**, 1029-1032.
4. C. Kuchinke, and M. Nunez, A variable sky-view platform for the measurement of ultraviolet radiation, *J. Atmos. Ocean Tech.*, 2003, **20**(8), 1170-1182.
5. A. Oppenrieder, P. Hoeppe and P. Koepke, Routine measurement of erythemally effective UV irradiance on inclined surfaces, *J. Photoch. Photobio. B.*, 2004, **74**, 85-94.
6. M. Mech and P. Koepke, Model for UV irradiance on arbitrarily oriented surfaces', *Theor. Appl. Climatol.*, 2004, **77**, 151-158.
7. B.L. Diffey, T.J. Tate and A. Davis, Solar dosimetry of the face: the relationship of natural ultraviolet radiation exposure to basal cell carcinoma localisation, *Phys. Med Biol.*, 1979, **24**, 931-939.
8. C.D.J. Holman, I.M. Gibson, M. Stephenson and B.K. Armstrong, Ultraviolet irradiation of human body sites in relation to occupation an outdoor activity: field studies using personal UVR dosimeters, *Clin. Exp. Dermatol.*, 1983, **8**, 269-277.
9. A. Milon, P. Sottas, J. Bulliard and D. Vernez, Effective exposure to solar UV in building workers: influence of local and individual factors, *J. Expo. Sci. Env. Epid.*, 2007, **17**, 58-68.
10. J.J. Streicher, W.C. Culverhouse, M.S. Dulberg and R.J. Fornaro, Modeling the anatomical distribution of Sunlight, *Photochem. Photobiol.* 2004, **79**, 40-47.
11. P. Hoeppe, A. Oppenrieder, C. Erianto, P. Koepke, J. Reuder, M. Seefeldner and D. Nowak, Visualization of UV exposure of the human body based on data from a scanning UV-measuring system', *Int. J. Biometeorology*, 2004, **49**, 18-25.
12. N.J. Downs and A.V. Parisi, Three dimensional visualisation of human facial exposure to solar ultraviolet, *Photochem. Photobiol. Sci*, 2007, **6**, 90-98.
13. NHMRC (National Health and Medical Research Council), Primary Prevention of Skin Cancer in Australia, Report of the Sun Protection Programs Working Party, Publication No. 2120, Australian Government Publishing Service, 1996.
14. P.H. Gies, C.R. Roy, S. Toomey, and A. McLennan, Protection against solar ultraviolet radiation, *Mutat. Res-Fund. Mol. M.*, 1998, **422**(1), 15-22.
15. NHMRC (National Health and Medical Research Council), Occupational Standard for Exposure to Ultraviolet Radiation, Radiation Health Series no. 29, Canberra, 1989.
16. NOHSC (National Occupational Health and Safety Commission), Guidance note for the protection of workers from ultraviolet radiation in sunlight, NOHSC: 3012., Australian Government, Canberra, October, 1991.
17. J.S. Greenwood, G.P. Soulos and N.D. Thomas, Under Cover: guidelines for shade planning and design, NSW Cancer Coucil, NSW Health Department, Sydney, 1998.
18. ARPANSA (Australian Radiation Protection and Nuclear Safety Agency), Radiation protection standard: occupational exposure to ultraviolet radiation, Regulatory Impact Statement, Australian Government, Canberra, 2006.

19. V.E. Cokkinides, K. Johnston-Davis, M. Weinstock, M.C. O'Connell, W. Kalsbeek, M.J. Thun and P.A. Wingo, Sun exposure and sun-protection behaviors and attitudes among U.S. youth, 11 to 18 years of age, *Prev. Med.*, 2001, **33**(3), 141-151.

20. P.M. Livingstone, V. White, J. Hayman and S. Dobbinson, Sun exposure and sun protection behaviours among Australian adolescents: trends over time, *Prev. Med.* 2003, **37**(6), 577-584.

21. M.A. Weinstock, G.A. Colditz, W.C. Willett, M.J. Stampfer, B.R. Bronstein and F.E. Speizer, Nonfamilial cutaneous melanoma incidence in women associated with sun exposure before 20 years of age, *Pediatrics*, 1989, **84**, 199-204.

22. J. Longstreth, F.R. de Gruijl, M.L. Kripke, S. Abseck, F. Arnold, H.I. Slaper, G. Velders, Y. Takizawa and J.C. van der Leun, Health Risks, *J. Photoch. Photobio. B.* 1998, **46,** 20-39.

23. A.F. Moise, P.G. Buttner and S.L. Harrison, Sun exposure at school, *Photochem. Photobiol.*, 1999, **70**(2), 269-274.

24. N.J. Downs, M.G. Kimlin, A.V. Parisi and J.J. McGrath, Modelling human facial UV exposure, *Radiat. Prot. Australas.* 2001, **17**(3), 103-109.

25. J.J. Michalsky, The astronomical almanac's algorithm for approximate solar position (1950-2050), *Solar Energy*, 1988, **40**, 227-235.

26. CIE (International Commission on Illumination), A reference action spectrum for ultraviolet induced erythema in human skin, *Comm. Int. Eclairage J.*, 1987, **6**(1), 17-22.

27. Total Ozone Mapping Spectrometer, 2008, National Aeronautics and Space Administration, viewed 27 March 2008, <http://jwocky.gsfc.nasa.gov/>

28. A.V. Parisi and N. Downs, Cloud cover and horizontal plane eye damaging solar UV exposures. *Int. J. Biomet.* 2004, **49,** 130-136.

29. R.D. Rundel, Computation of spectral distribution and intensity of solar UVB radiation, in *Stratospheric Ozone Reduction, Solar Ultraviolet Radiation and Plant Life*, eds. R.C. Worrest and M.M. Caldwell, Springer-Verlag, 1986, Berlin.

30. P.F. Schippnick and A.E.S. Green, Analytical characterization of spectral actinic flux and spectral irradiance in the middle ultraviolet, *Photochem. Photobiol.*, 1982, **35**, 89-101.

31. A.E.S. Green, T, Sawada and E.P. Shettle, The middle ultraviolet reaching the ground, *Photochem. Photobiol.* 1974, **19**, 251-259.

32. M.G. Kimlin, N.J. Downs and A.V. Parisi, Comparision of human UV facial exposure at high and low latitudes and the potential impact on dermal vitamin D production, *Photochem. Photobiol. Sci.* 2003, **2** 370-375.

33. A.E.S. Green, K.R. Cross and L.A. Smith, Improved analytic characterization of ultraviolet skylight, *Photochem. Photobiol.* 1980, **31**, 59-65.

34. B.L. Diffey, C.T. Jansen, F. Urbach and H.C. Wulf, The standard erythema dose: a new photobiological concept, *Photodermatol. Photoimmunol. Photomed.* 1997, **13,** 64-66.

35. N. Downs and A. Parisi, Patterns in the received facial UV exposure of school children measured at a subtropical latitude, *Photochem. Photobiol.* 2008, **84**(1), 90-100.

36. D.J. Turnbull and A.V. Parisi, Effective shade structures, *Med. J. Aus.*, 2006, **184**, 13-15.

37. C.F. Wong, Scattered ultraviolet radiation underneath a shade-cloth, *Photodermatol. Photoimmunol. Photomed.* 1994, **10**, 221-224.

38. S.J. Toomey, H.P. Gies and C.R. Roy, UVR protection offered by shadecloths and polycarbonates, *Rad. Prot. Dos. Aust*. 1995, **13**(2), 50-54.
39. P. Gies and C. Mackay, Measurements of the solar UVR protection provided by shade structures in New Zealand primary schools, *Photochem. Photobiol.* 2004, **80**, 334-339.
40. G.M. Heisler, R.H. Grant and W. Gao, Individual- and scattered-tree influences on ultraviolet irradiance, *Agr. Forest Meteorol.*, 2003, **120**, 113-126.
41. A.V. Parisi and M.G. Kimlin, Comparison of the spectral biologically effective solar ultraviolet in adjacent tree shade and sun, *Phys. Med. Biol.* 1999, **44**, 2071-2080.
42. A.V. Parisi, M.G. Kimlin, J.C.F. Wong and M. Wilson, Solar ultraviolet exposures at ground level in tree shade during summer in south east Queensland, *Int. J. Environ. Heal. R.*, 2001, **11**, 117-127.
43. M.F. Holick, Evolution and function of vitamin D, *Recent Res. Cancer*, 2003, **164**, 3-28.
44. E. Hypponen, E. Laara and A. Reunanen, Intake of vitamin D and risk of type 1 diabetes: a birth-cohort study, *Lancet*, 2001, **358**, 1500-1503.
45. C.E. Hayes, M.T. Cantorna and H.F. DeLuca, Vitamin D and multiple sclerosis, *Proc. Soc. Exp. Biol. Med.*, 1997, **216**, 21-27.
46. E.D. Gorham, F.C. Garland and C.F. Garland, Sunlight and breast cancer incidence in the USSR, *Int. J. Epidemiol.*, 1990, **19**, 614-622.
47. C. Garland, F.C. Garland, E.D. Gorham, M. Lipkin, H. Newmark, M.F. Holick, J.V. Raffa, Ultraviolet B, vitamin D, and their mechanisms in cancer prevention, in *Ultraviolet Ground- and Space-based Measurements, Models, and Effects: Proceedings of SPIE*, eds. J.R. Slusser, J.R. Herman, and W. Gao, The International Society for Optical Engineering, SPIE, Bellingham, WA. 2002, pp. 313-323.
48. W.B. Grant, An estimate of premature cancer mortality in the U.S. due to inadequate doses of solar UV-B radiation, *Cancer*, 2002, **94**, 1867-1875.
49. J.J. McGrath, Does 'imprinting' with low prenatal vitamin D contribute to the risk of various adult disorders?, *Med. Hypotheses*, 2001, **56**, 367-371.